Atmospheric
Chemistry
and Physics
Discussions

1 **Zeppelin-led study on the onset of new particle formation in the planetary boundary layer**

2

3 Janne Lampilahti[1], Hanna E. Manninen[2], Tuomo Nieminen[1], Sander Mirme[3], Mikael Ehn[1], Iida

4 Pullinen[4], Katri Leino[1], Siegfried Schobesberger[1,4], Juha Kangasluoma[1], Jenni Kontkanen[1], Emma

5 Järvinen[5], Riikka Väänänen[1], Taina Yli-Juuti[4], Radovan Krejci[6], Katrianne Lehtipalo[1,7], Janne

6 Levula[1], Aadu Mirme[3], Stefano Decesari[8], Ralf Tillmann[9], Douglas R. Worsnop[1,4,10], Franz Rohrer[9],

7 Astrid Kiendler-Scharr[9], Tuukka Petäjä[1,11], Veli-Matti Kerminen[1], Thomas F. Mentel[9], and Markku

8 Kulmala[1,11,12]

9

10 [1]Institute for Atmospheric and Earth System Research / Physics, Faculty of Science, University of

11 Helsinki, Helsinki, Finland.

12 [2]CERN, CH-1211 Geneva, Switzerland.

13 [3]Institute of Physics, University of Tartu, Tartu, Estonia.

14 [4]Department of Applied Physics, University of Eastern Finland, Kuopio, Finland.

15 [5]National Center for Atmospheric Research, Boulder, CO, USA.

16 [6]Department of Environmental Science & Bolin Centre for Climate research, Stockholm University,

17 Stockholm, Sweden.

18 [7]Finnish Meteorological Institute, Helsinki, Finland.

19 [8]Istituto di Scienze dell'Atmosfera e del Clima, CNR, Bologna, Italy.

20 [9]Institute for Energy and Climate Research, IEK-8, Forschungszentrum Jülich GmbH, Jülich,

21 Germany.

22 [10]Aerodyne Research Inc, Billerica, MA, USA.

23 [11]Joint International Research Laboratory of Atmospheric and Earth System Sciences, Nanjing.

24 University, Nanjing, China.

25 [12]Aerosol and Haze Laboratory, Beijing Advanced Innovation Center for Soft Matter Science and

26 Engineering, Beijing University of Chemical Technology, Beijing, China.

27

28 Correspondence to: Janne Lampilahti (janne.lampilahti@helsinki.fi)

29

30 **Abstract**

31 We compared observations of aerosol particle formation and growth in different parts of the

32 planetary boundary layer at two different environments that have frequent new particle formation

33 (NPF) events. In summer 2012 we had a campaign in Po Valley, Italy (urban background) and in

34 spring 2013 a similar campaign took place in Hyytiälä, Finland (rural background). Our study

35   consists of airborne and ground-based measurements of ion and particle size distribution from ~1

36   nm. The airborne measurements were performed using a Zeppelin inside the boundary layer up to

37   1000 m altitude. Our observations show the onset of regional NPF and the subsequent growth of the

38   aerosol particles happening uniformly inside the mixed layer (ML) in both locations. However, in

39   Hyytiälä we noticed local enhancement in the intensity of NPF caused by mesoscale BL dynamics.

40   Additionally, our observations indicate that in Hyytiälä NPF was probably also taking place above

41   the ML. In Po Valley we observed NPF that was limited to a specific air mass.

42

43   **1 Introduction**

44   The boundary layer (BL) is the lowest layer of the earth's atmosphere (Stull, 1988). The BL is an

45   interface controlling the exchange of mass and energy between atmosphere and surface. Ground

46   based measurements are often used as representative observations for the whole BL. However they

47   cannot cover vertical internal variability of BL and this can be addressed only by airborne

48   observations.

49

50   Figure 1 show the typical BL evolution over land during the time span on one day. Shortly after

51   sunrise convective mixing creates a mixed layer (ML) that rapidly grows during the morning by

52   entraining air from above and can reach an altitude of ~1-2 km above the surface. The ML is capped

53   by a stable layer at the top. Above the BL is the free troposphere (FT), which is decoupled from the

54   surface. Here we define BL to mean all the layers below the FT. Around sunset convective mixing

55   and turbulence diminishes and the ML becomes what is known as the residual layer (RL). During

56   the night a stable boundary layer develops due to interaction with the ground surface. This layer has

57   only weak intermittent turbulence and it smoothly blends into the RL.

58

59   We studied where new particle formation (NPF) occurs in the BL and how it relates to BL

60   evolution, comparing two different environments. NPF refers to the formation of nanometer sized

61   clusters from low-volatility vapors present in the atmosphere, and their subsequent growth to larger

62   aerosol particles (Kulmala et al., 2013). Understanding NPF better is of major interest, since it is a

63   dominant source of cloud condensation nuclei in the atmosphere and therefore can have important

64   indirect effects on climate (Dunne et al., 2016; Gordon et al., 2017; Pierce and Adams, 2009; Yu and

65   Luo, 2009).

66

67   Nilsson et al. (2001) studied NPF in a boreal forest environment and observed that in addition to

68   increased solar radiation the onset of turbulence appears to be a necessary trigger for NPF. Several

69 explanations for this connection were proposed: NPF might be starting in the RL or at the top of the

70 shallow ML, from where the aerosol particles are mixed to the surface as the ML starts to grow.

71 NPF starts in the ML due to dilution of pre-existing aerosol and drop in vapor sink. Convective

72 mixing brings different precursor gases, one present in the RL and the other in the ML, into contact

73 with each other initiating NPF inside the ML.

74

75 Airborne measurements of nanoparticles from different environments show that NPF occurs in

76 many parts of the BL. Multiple observations from Central Europe suggest that aerosol particles are

77 formed on top of a shallow ML (Platis et al., 2015; Siebert et al., 2004; Chen et al., 2018) or inside

78 the RL (Stratmann et al., 2003; Wehner et al., 2010). Other results come from a boreal forest

79 environment in southern Finland. Lampilahti et al. (2020a) showed evidence that NPF may occur in

80 the interface between the RL and the FT. O'Dowd et al. (2009) observed the first signs of NPF in

81 the surface ML and Leino et al. (2019) showed that sub-3 nm particles have higher concentration

82 close to surface. Laakso et al. (2007) performed hot-air balloon measurements and concluded that

83 NPF either took place throughout the ML or in the lower part of the ML. Measurements by

84 Schobesberger et al. (2013) suggested that NPF was more intense in the top parts of a developed

85 ML. More measurements are needed in order to understand these mixed results.

86

87 Here we present NPF measurements on board a Zeppelin airship carried out during the EU

88 supported PEGASOS (Pan-European Gas-AeroSOls Climate Interaction Study) project. The main

89 goal of the project was to quantify the magnitude of regional to global feedbacks between

90 atmospheric chemistry and physics, and thus quantify their impact on the changing climate. The

91 Zeppelin flights were used to observe radicals, trace gases, and aerosol particles inside the lower

92 troposphere over Europe in several locations during 2012-2013.

93

94 By using a Zeppelin NT (Neue Technologie) airship we were able to sample from a stable, agile

95 platform, up to 1000 meters above sea level (asl). The high payload capacity of the Zeppelin

96 enabled us to carry state-of-the-art instrumentation, specifically designed to collect information on

97 the feedback processes between the chemical compounds and the smallest aerosol particles to better

98 estimate their role in climate and air quality.

99

100 The NPF focused campaigns presented here were performed in Po Valley, Italy, and Hyytiälä,

101 Finland. At both locations NPF events happen frequently. Po Valley represents urban background

102 conditions where anthropogenic emissions are an important source of gaseous precursors for NPF

103   (e.g. Kontkanen et al., 2016). Hyytiälä represents rural background conditions where organic vapors

104   from the surrounding forests play a major role in NPF (e.g. Dada et al., 2017).

105

106   Here we combine comprehensive ground-based and airborne measurements to compare two NPF

107   cases from Po Valley to one case from Hyytiälä. The Zeppelin allowed us to repeatedly profile the

108   lowest 1 km of the atmosphere providing a full picture of what is happening in the BL during the

109   onset of NPF. We will show in which part or parts of the BL the onset of NPF and the subsequent

110   particle growth occurred at the two measurement sites as well as determine formation and growth

111   rates for the aerosol particles.

112

113   **2 Methods**

114   San Pietro Capofiume in Po Valley, Italy and Hyytiälä in Southern Finland are interesting

115   environments to compare from nucleation and particle growth point of view because NPF is

116   frequently observed in both environments. The vertical measurement profiles analyzed in this study

117   were performed in a close proximity to the ground-based measurement sites.

118

119   **2.1 San Pietro Capofiume, Italy**

120   San Pietro Capofiume (SPC, 44°39'N 11°37'E, 11 m asl) is located in the eastern part of Po Valley,

121   Italy, between the cities of Bologna and Ferrara. Po Valley is considered a pollution hot spot,

122   although, the station itself is surrounded by vast agricultural fields away from point sources. Thus

123   the aerosol concentration and composition at SPC reflect the Po Valley regional background. NPF is

124   frequently observed in SPC (36% of days) with maxima in May and July (Hamed et al., 2007;

125   Laaksonen et al., 2005).

126

127   The instruments measuring the aerosol particle number-size distribution were a scanning mobility

128   particle sizer (SMPS, 10-700 nm, 5 min time resolution; Wiedensohler et al., 2012) and a neutral

129   cluster and air ion spectrometer (NAIS, particles: ~2-40 nm, ions: 0.8-40 nm, 4 min time resolution;

130   Mirme and Mirme, 2013). We used the NAIS's positive polarity for the particle number size

131   distribution data. The ML height was determined from ceilometer (Lufft CHM 15k) measurements.

132   Basic meteorology and SO_2 gas concentration data (Thermo 43iTLE monitor) were also available at

133   surface level (2-3 m above ground level).

134

135   **2.2 Hyytiälä, Finland**

136   In Finland the ground-based measurements were performed at the SMEAR II (Station for

137   Measuring Forest Ecosystem-Atmosphere Relations II) station located in Hyytiälä, Finland (HTL,

138   61°51'N 24°17'E, 181 m asl; Hari and Kulmala, 2005). The station is equipped with extensive

139   facilities to measure the forest ecosystem and the atmosphere. The measurement site is surrounded

140   by coniferous boreal forest.

141

142   The forest emits biogenic volatile organic compounds (Hakola et al., 2003), which can be oxidized

143   in the atmosphere to form low-volatile vapors that contribute to aerosol particle formation and

144   growth (Ehn et al., 2014; Mohr et al., 2019). NPF is frequently observed in HTL (23% of all days),

145   especially in spring and autumn (Dal Maso et al., 2005; Nieminen et al., 2014).

146   Aerosol particle and ion number-size distributions were measured by the station's differential

147   mobility particle sizer (DMPS, 3-1000 nm, 10 min time resolution; Aalto et al., 2001) and the NAIS

148   (Manninen et al., 2009). Sub-3 nm particle number-size distribution was measured by a particle size

149   magnifier running in scanning mode (PSM, 1.2-2.5 nm, 10 min time resolution; Vanhanen et al.,

150   2011). Also a PSM measured at SPC but we were not able to reliably calculate formation rates from

151   the data. Basic meteorological variables, radiation, and SO_2 were measured from the station's mast

152   at 16.8 meters above ground. In addition, a supporting NPF forecast tool was developed to aid the

153   planning of research flights (Nieminen et al., 2015).

154

155   **2.3 Zeppelin NT airship**

156   A Zeppelin NT airship was used for monitoring the atmosphere below 1 km. The aerosol particles

157   and trace gases were sampled with instrumentation installed inside the Zeppelin's cabin. The

158   Zeppelin operated with three different instrument layouts. A specific layout was chosen according to

159   the flight plan and scientific aim of the flight.

160

161   Here we analyzed data from measurement flights that carried the so-called nucleation layout.

162   Instruments specific to this layout were the atmospheric pressure interface time-of-flight mass

163   spectrometer (APi-TOF; Junninen et al., 2010), used for measuring the elemental composition of

164   naturally charged ions and the NAIS for particle and ion number size distributions. We also used the

165   aerosol number-size distribution data from the SMPS (10-400 nm, 4 min time resolution) and PSM

166   running in scanning mode, which were on board during all the measurement flights. The size range

167   and time resolution of the onboard NAIS and PSM were same as for the instruments in HTL (see

168   Section 2.1).

169

170 During a measurement flight the Zeppelin did multiple vertical profiles over a small area (~10 km^2).

171 The profiling spot was picked typically down-wind from the measurement site in order not to

172 compromise the ground-based measurements with any emissions. The vertical extent of the profiles

173 was ~100-1000 m above the ground. The airspeed during measurement was ~20 m/s and the

174 vertical speed during ascend and descend was ~0.5 m/s and ~3 m/s respectively.

175

176 **2.4. Cessna 172 airplane**

177 During the PEGASOS northern mission in spring 2013, a Cessna 172 airplane carrying scientific

178 instrumentation was deployed to measure aerosol particles, trace gases and meteorological variables

179 in the lower troposphere alongside the Zeppelin. The measurement setup and instrumentation on

180 board have been described in previous studies (Schobesberger et al., 2013; Lampilahti et al., 2020c;

181 Leino et al., 2019; Väänänen et al., 2016).

182

183 Basic meteorological variables (temperature, pressure, relative humidity) were measured on board.

184 Particle number-size distribution was measured using a SMPS (10-400 nm size range, 2 min time

185 resolution) and the number concentration of >3 nm particles was measured using an ultrafine

186 condensation particle counter (UF-CPC, TSI model 3776) at 1 s time resolution. The altitude range

187 of the airplane was ~100-3000 m above ground and the measurement airspeed was 36 m/s.

188

189 **2.5 Flight profiles and atmospheric conditions**

190 Our measurements focused on the time of BL development from sunrise until noon (Figure 1). This

191 is the time when the onset of NPF is typically observed at the ground level. The vertical profile

192 measurements represent the particle and gas concentrations in the lower parts of the atmosphere: the

193 mixed layer, the residual layer, the nocturnal boundary layer. At the same time, the ground-based

194 measurements recorded conditions in the surface layer. Here we consider the BL to include all the

195 atmospheric layers below the free troposphere.

196

197 The basic conditions for the Zeppelin flights in both Italy and Finland were clear sky and low wind

198 speed. Under these conditions, the sun heats the surface during the morning, which drives intense

199 vertical mixing.

200

201 **2.6 Data analysis**

202 The onset of NPF occurs when low-volatility vapors in the atmosphere form nanometer sized

203 clusters that continue to grow to larger aerosol particles (Kulmala et al., 2013).

204

205   We determined the onset of a NPF event visually from the initial increase in the number

206   concentration of intermediate (2-4 nm) air ions at the beginning of the NPF event. An increase in

207   the intermediate ion concentration has been identified as a good indicator for NPF (Leino et al.,

208   2016). This is because an increase in the number concentration of intermediate ions is usually due

209   to NPF and otherwise the number concentration is extremely low (below 5 cm^{-3}).

210

211   Particle growth rates (GR), formation rates and coagulation sinks were calculated in different size

212   ranges according to the methods described by Kulmala et al. (2012). For particles and ions in the 1-

213   2 nm and 2-3 nm size range the GR was determined from the ion number-size distribution measured

214   by the NAIS. During NPF the number concentration in each size channel increased sequentially as

215   the freshly formed particles grew larger. We determined the time when the number concentration

216   began to rise in each size bin by fitting a sigmoid function to the rising concentration edge and

217   finding the point where the sigmoid reached 75% of its maximum value (appearance time method;

218   Lehtipalo et al., 2014). The corresponding diameter in each size bin was the bin's geometric mean

219   diameter. Before the fitting procedure the number concentrations were averaged using a 15 min

220   median and after that divided by the maximum concentration value in each size channel.

221

222   For larger particles and ions (3-7 nm and 7-20 nm) the GR was determined by fitting a log-normal

223   distribution over the growing nucleation mode at each time step and assigning the fitted curve's

224   peak value as the corresponding mode diameter. In each size range a value for the GR was obtained

225   as the slope of a linear least squares fit to the time-diameter value pairs.

226

227   The formation rate of 1.5 nm particles and ions was determined from the PSM data and the NAIS

228   ion data respectively (Kulmala et al., 2012). The formation rate of 3 nm particles and ions was

229   determined from the NAIS data. Coagulation sinks were calculated from the SMPS or DMPS data.

230   Condensation sink for sulfuric acid was calculated from the Zeppelin's on board SMPS.

231

232   Sulfuric acid (SA) is a key compound in atmospheric nucleation (Sipilä et al., 2010). As we did not

233   have direct measurements of SA concentration, we used [HSO4-] from the APi-TOF measurements

234   as a qualitative indicator of [H2SO4] and named it pseudo-SA. To determine this pseudo-SA, we

235   summed up all ions containing HSO4-, e.g. the ion itself but also larger clusters, like

236   (H2SO4)$_n$*HSO4-. We assumed steady state conditions and that the concentration of SA-containing

237   ions is much lower than the total ion concentration. Under these conditions [HSO4-] (including all

238   clusters where this ion was present) can be considered close to a linear function of [H2SO4] (Eisele

239   and Tanner, 1991). At the highest SA loadings, ions with HSO4- can be a dominant fraction of the

240   total ions (Ehn et al., 2010), in which case the linearity no longer holds. In addition, this assumes a

241   constant concentration of ions, although for example the sinks for ions can vary, e.g. by an

242   increased particle concentration. As such, the pseudo-SA parameter should indeed only be

243   considered a qualitative indicator for SA.

244

245   In SPC the ML height was derived from the ceilometer measurements. However, in HTL weak

246   scattering signal prevented reliable determination of ML height using the on-site lidar. For this

247   reason in HTL the ML height was determined from vertical profiles of meteorological variables and

248   aerosol particle concentrations on board the Zeppelin and the Cessna 172 airplane. In these profiles

249   the top of the ML was revealed by the maximum positive gradient in potential temperature and

250   minimum negative gradient in humidity and total particle number concentration (Stull, 1988).

251

252   The origin of the air masses was investigated using back trajectory analysis. The trajectories were

253   calculated with the HYSPLIT (Hybrid Single Particle Lagrangian Integrated Trajectory; Stein et al.,

254   2015) model using the GDAS (Global Data Assimilation System) archived data sets.

255

256

257   **3 Results and discussion**

258

259   **3.1 Case study description**

260   During the campaigns there were a limited number of flights with the nucleation instrument

261   payload. Here we present a side by side comparison of two case studies, one from SPC (June 28,

262   2012) and the other from HTL (May 8, 2013). In addition the horizontal extent of NPF in SPC was

263   investigated by studying the research flight from June 30, 2012.

264

265   June 28, 2012 was a hot and sunny day in Po Valley. 24-h back trajectories arriving to SPC during

266   the morning revealed that the incoming air masses circulated from Central Europe and over the

267   Adriatic Sea before arriving to SPC from the southwest (Figure 2a). Figure 3 shows the time series

268   for some environmental parameters on the NPF event days from SPC and HTL. In SPC temperature

269   and RH showed a large diurnal variation; the temperature increased from 16 °C to 32 °C during the

270   morning while the RH decreased from 87% to 39%. The mean wind speed at 10 m height was 2.0 m

Atmospheric
Chemistry
and Physics
Discussions

Open Access

EGU

271 s^{-1}. These meteorological conditions and air mass histories are common during NPF event days in

272 Po Valley (Hamed et al., 2007; Sogacheva et al., 2007).

273

274 May 8, 2013 in HTL was a sunny and warm day with clear skies marked by broad diurnal variation

275 in temperature and RH. During the morning the temperature increased from 5 °C to 17 °C and the

276 RH decreased from 82% to 25%. The mean wind speed at 33.6 m height was 3.5 m s^{-1}. The air

277 masses originated from the North Atlantic Ocean arriving to HTL from the northwest via

278 Scandinavia and the Gulf of Bothnia (Figure 2b). Most NPF event days in HTL are clear sky days

279 with the arriving air masses spending most of their time in the northwest sector (Dada et al., 2017;

280 Nilsson et al., 2001; Sogacheva et al., 2008).

281

282 In SPC the solar radiation began to increase after 04:00 and the ML started to increase in height

283 around 06:00, at the same time the SO_2 concentration and $N_{>10}$ (number concentration of particles

284 larger than 10 nm) began to increase. This is likely explained by the entrainment of pollutants from

285 the RL and the onset of NPF. CS is higher during the night and decreases slightly during the day,

286 which is likely due to dilution related to ML growth.

287

288 At HTL after sunrise the SO_2 concentration and $N_{>10}$ decreased probably due to the dilution caused

289 by the growing ML coupled with the lack of pollution sources. While SO_2 concentration remained

290 low the whole day, $N_{>10}$ and CS began to increase later during the day because of the NPF event.

291 The average SO_2, $N_{>10}$ and CS in SPC were 0.57 ppb, 8102 cm^{-3} and 0.0128 s^{-1} respectively. While

292 in HTL the corresponding values were 0.02 ppb, 3293 cm^{-3} and 0.0007 s^{-1}.

293

294 **3.2 Onset of NPF**

295 Figures 4a and 4b show the altitude of the Zeppelin as a function of time colored by the number

296 concentration of intermediate ions measured by the NAIS at SPC and HTL. The plots also show the

297 number concentration of intermediate ions measured on the ground as well as the ML height.

298

299 In SPC, the intermediate ion concentration began to increase on the ground at 5:48, which coincides

300 with the beginning of convective mixing and the breakup of the nocturnal surface layer. Similarly,

301 Kontkanen et al. (2016) observed that in Po Valley the onset of NPF coincided with the beginning

302 of boundary layer growth. Around this time the Zeppelin was profiling the layers above the ML.

303 "Pockets" of elevated intermediate ion concentration were present inside the RL (for example

304 around 700 m at 5:15). These pockets were not linked to the NPF event inside the ML. When the

305   Zeppelin later entered the ML at around 6:45, NPF was already taking place throughout the

306   developing ML and seemed to be confined to it.

307

308   In HTL, the number concentration of intermediate ions began to increase at around 6:47 on the

309   ground level. The ML at this point had grown to around 600 m above ground, which allowed us to

310   better resolve the onset of NPF vertically. In HTL no increase in intermediate ion concentration,

311   indicating no NPF, was observed above the ML on board the Zeppelin. Before 6:40 there was no

312   sign of NPF inside the growing ML. Between 6:40 and 7:00 the Zeppelin briefly measured in the

313   RL and re-entered the ML at 7:00. At this point the intermediate ion concentration was already

314   increasing on board similar to the ground level, indicating the onset of NPF.

315

316   Figure 5 shows the intermediate ion number concentration as a function of time from the Zeppelin

317   and the SMEAR II station. At the beginning of the NPF event, between 07:00-07:15, the Zeppelin

318   ascended from 300 m to 800 m. During the ascend the intermediate ion concentrations increased at

319   a similar rate and stayed at similar values on board the Zeppelin and at the ground level. The lack of

320   vertical gradient in the number concentration suggests that the aerosol particles were forming

321   homogeneously throughout the ML. However, intense turbulent mixing and strong updrafts moving

322   up at roughly the same rate as the Zeppelin might have also resulted in a homogeneous number

323   concentration, even if the aerosol particles were formed close to the surface.

324

325   Figures 4c and 4d show the Zeppelin's measurement profiles colored with the pseudo SA. In SPC,

326   the highest amount of pseudo SA appears to be in the residual layer above the growing morning ML

327   (also observed on June 27, 2012) after sunrise. This is in line with the observation that the SO_2

328   concentration increases at the surface when the ML starts to grow (Figure 3b), indicating that the

329   SO_2 was entrained from the RL. The entrainment of SO_2 from the residual layer is also supported by

330   previous observations (Kontkanen et al., 2016). The increased pseudo SA in the residual layer was

331   not associated with NPF in the residual layer.

332

333   In SPC the night time SO_2 concentration at the surface is low likely due to deposition (Kontkanen et

334   al., 2016). However ammonia concentration can be high (>30 μg m^{-3}) at the surface due to

335   agricultural activities and the concentration has been observed to peak during the night and early

336   morning (Sullivan et al., 2016).

337

371   We calculated the formation and growth rates in SPC and HTL for particles and ions on board the

372   Zeppelin and on the ground. The results are summarized in Table 1. In SPC the onset of NPF

373   happened when the ML was still very shallow and the Zeppelin was not measuring significant

374   amount of time at this low altitude (this was a problem on other NPF event days from SPC as well),

375   consequently the beginning of the NPF event was not fully observed on board. Because of this we

376   were unable to reliably calculate the formation rates and the growth rate between 1-2 nm from the

377   Zeppelin data.

378

379   Kontkanen et al. (2016) obtained formation rates of 23.5 cm^{-3} s^{-1}, 9.5 cm^{-3} s^{-1}, 0.1 cm^{-3} s^{-1} and 0.08

380   cm^{-3} s^{-1} for 1.5 nm particles, 2 nm particles, 2 nm positive ions and 2 nm negative ions respectively

381   for the June 28, 2012 NPF event at the ground level. These values are in line with our values for the

382   same day reported in Table 1 (J_3 = 6.8 cm^{-3}, J_3^- = 0.04 cm^{-3}, J_3^+ = 0.03 cm^{-3}). The higher formation

383   rates in SPC compared to HTL are characteristic of polluted environments (Kerminen et al., 2018).

384   The calculated GRs for the larger particle sizes as seen in Table 1 were similar on board the

385   Zeppelin (HTL: GR_{7-20} = 2.4 nm/h, SPC: GR_{7-20} = 3.0 nm/h) and on the ground (HTL: GR_{7-20} = 2.1

386   nm/h, SPC: GR_{7-20} = 2.8 nm/h).

387

388   On May 8, 2013 in HTL almost the whole NPF event was captured by the Zeppelin measuring

389   inside the ML. However, in contrast to SPC the number size distributions measured on board the

390   Zeppelin (Figure 6b) and on the ground (Figure 6d) show differences, particularly in the growing

391   nucleation mode particles. At different times on board the Zeppelin when it was measuring inside

392   the ML the particle number concentration in the growing mode momentarily increased up to eight

393   fold compared to the background number concentration, suggesting an enhancement in the particle

394   formation rate. On board the Zeppelin this can be seen as concentrated "vertical stripes" in the

395   number size distribution between 08:00-10:00. On the other hand at the ground station an increase

396   of concentration of freshly formed particles was observed between 7:30-8:00. This inhomogeneity

397   is further discussed in Section 3.3.

398

399   In the ground-based NAIS data a pool of sub-6 nm particles was present during the NPF event

400   while on board the Zeppelin no such pool was observed. This can be seen most clearly between

401   10:00-11:30 when the median particle number concentration between 2-4 nm on the ground was

402   1400 cm^{-3} whereas on board the Zeppelin it was 570 cm^{-3}. Similarly Leino et al. (2019) observed

403   that the number concentration of sub-3 nm particles decreases as a function of altitude at HTL. This

404   may be linked to increased concentration of low-volatility vapors on the surface near the sources

405   compared to aloft.

406

407   Despite the differences in the ground-based and airborne number size distributions in HTL a

408   continuous, growing, nucleation mode was observed in the "background" both on the ground

409   (alongside the pool of sub-6 nm particles) and on board the Zeppelin during the NPF event. When

410   averaged over the total duration of the NPF event, the growth rates and formation rates on board the

411   Zeppelin and on the ground were similar on this day. This would indicate that the ground-based

412   measurements represent the NPF event in the whole ML quite well. However locally increased

413   number concentrations, indicating enhanced NPF, were observed inside the ML and if the

414   enhancement is not detected with the ground-based measurements we may underestimate the

415   intensity of NPF within the ML based on ground-based data alone.

416

417   **3.3 Vertical and horizontal distribution of the freshly formed particles**

418   Next we investigated how the freshly formed particles were distributed spatially in the BL. Figure 7

419   shows the particle number concentration between 3-10 nm measured by the NAIS and the ML

420   height from SPC as a function of time and altitude. The freshly formed particles were distributed

421   homogeneously throughout the growing ML but were not found in the RL. The 3-10 nm number

422   concentration inside the ML was ~20 000 cm^{-3} while in the residual layer it was only ~200 cm^{-3}. The

423   pockets of increased intermediate ion concentration, indicating NPF in the nocturnal boundary layer

424   and residual layer (Figure 4a), were not observed in the 3-10 nm size range suggesting that the

425   particles did not grow to the 3-10 nm size range in any significant numbers.

426

427   At HTL the Zeppelin was measuring in the lower half of the developed ML, however the Cessna

428   profiled the entire depth of the ML all the way up to the lower parts of the free troposphere. Figure

429   8 shows the vertical profile of 3-10 nm particle number concentration between 07:00-10:00 UTC

430   calculated by subtracting the total SMPS number concentration from the UF-CPC number

431   concentration on board the Cessna. Also the water vapor concentration and temperature are shown.

432   A temperature inversion, a large negative gradient in water vapor concentration and in the particle

433   number concentration indicated that the top of the ML was present between 1300-1400 m.

434

435   On average the number concentration inside the ML remained roughly constant (N_{3-10} ~1000 cm^{-3})

436   as a function of altitude, however there was substantial variation (~200-3000 cm^{-3}). The strongest

437   variation came from a narrow sector roughly at the center of the measurement area, which is

13

438   discussed below. The NPF did not extend to the RL where the number concentrations were reduced

439   to below 100 cm^{-3}.

440

441   However at 2000 m a layer of sub-10 nm particles was observed. The 3-10 nm number

442   concentration increased from less than 100 cm^{-3} to ~400 cm^{-3}. Lampilahti et al. (2020a) showed

443   evidence that NPF frequently takes place in the interface between the residual layer and the free

444   troposphere, disconnected from the ML. Precursor gases may be transported to these altitudes and

445   the mixing over the interface layer could initiate nucleation.

446

447   Figure 9a shows the particle number concentration between 3-10 nm on board the Zeppelin and the

448   airplane as a function of longitude and latitude from HTL on May 8, 2013. The particle number

449   concentration was elevated right over HTL in a narrow sector perpendicular to the mean wind

450   direction. Vertically the sector extended throughout the depth of the ML. The number concentration

451   in the sector increased 2-8 fold compared to the surrounding background number concentration. The

452   mean wind speed in the ML was about 4 m/s and the particle sector was observed throughout the

453   whole measurement flight, for at least 2.5 hours. This suggests that the particle sector was probably

454   at least 35 km long along the mean wind direction.

455

456   The concentrated vertical stripes over the growing nucleation mode in Figure 6b were caused by the

457   Zeppelin periodically flying through the particle sector. The sector slowly moved perpendicular to

458   the mean wind towards northeast and when passing over HTL it was seen as the plume of particles

459   in Figure 6d between 07:30-08:00. The particles in the sector grew at approximately the same rate

460   with the background NPF event particles, which also suggests that the particles were formed

461   simultaneously inside the long and narrow sector. Lampilahti et al. (2020b) showed that these types

462   of NPF events, or local enhancements of regional NPF events, are common in HTL and that they

463   are linked to roll vortices, which are a specific mode of organized convection in the BL.

464

465   On June 28, 2012 in SPC the Zeppelin flew the measurement profiles over a small area and

466   therefore it was difficult to infer the horizontal extent of the NPF event. However, on June 30, 2012

467   the Zeppelin measured over a larger area in order to find the edges of the airmass where the NPF

468   event was taking place. The flight on June 30, 2012 lasted from 05:00 to 10:00 UTC. Figure 9b

469   shows that the NPF event was observed to occur in the sector of the Valley comprised between

470   Ozzano (just north of the Apennine foothills) and the city of Ferrara (just south of the Po river). The

14

471 area in between experienced westerly winds, from the inner Po Valley toward the Adriatic sea,

472 which is a common feature of the Po Valley wind breeze system in the early morning.

473

474 Farther north of the Po river, an easterly breeze was developing and no NPF was observed (off the

475 map in Figure 9b, see Figure 10). Nocturnal north-easterly breezes are often observed over the

476 Three Venezie Plain as a result of a low-level jet (Camuffo et al., 1979). The variability in local

477 wind fields may generate chemical gradients in the atmospheric surface layer within the Po Valley,

478 hence segregating air masses which can be active or inactive with respect to NPF, in complete

479 absence of orographic forcings (i.e. over a completely flat terrain). Probably the air masses with an

480 easterly component reaching the Zeppelin from the Venetian plain picked up pollution (e.g. CO,

481 NO_x) from urban sources, but we can also speculate that for example ammonia and amines were

482 much lower than in the westerly air masses flowing south of the Po river, which had crossed the

483 areas between Emilia and Lombardy where most agricultural activities take place (see Figure 10). A

484 chemical transport model run predicting NH_3 concentrations with adequate resolution, and using

485 them as a tracer for the actual precursors for NPF, might clarify this point. However modeling

486 atmospheric transport at this scale in an environment like Po Valley can have substantial

487 uncertainties (Vogel and Elbern, 2021).

488

489

490 **4 Conclusions**

491

492 Flight measurements are essential to evaluate the representativeness of the ground-based in-situ

493 measurements. In many cases it may be impossible to tell from only ground-based data what drives

494 the observed NPF, especially when the effect of BL dynamics is important. Atmospheric models

495 require field observations for validation and constraints. Airborne measurements such as the ones

496 reported here provide valuable data for this purpose.

497

498 We compared two different environments where NPF occurs frequently: a suburban area in Po

499 Valley, Italy, and a boreal forest in Hyytiälä, Finland. We aimed to answer in which part of the BL

500 the onset of NPF and the growth of the freshly formed particles takes place and studied the vertical

501 and horizontal extent of NPF.

502

503 To detect directly the very first steps of NPF in the BL, we used airborne Zeppelin and airplane

504 measurements, supported by ground-based in-situ measurements. The Zeppelin measurements

Atmospheric
Chemistry
and Physics
Discussions

505   allowed us to study the vertical extent of NPF in the BL. The high time resolution and low cut-off

506   size of the instruments on board allowed us to observe the starting time, location and altitude of an

507   NPF event.

508

509   Within the limits of the Zeppelin's vertical profiling speed (~ 0.5 m/s ascend) and the time

510   resolution of the NAIS, we observed that the onset of NPF happened simultaneously inside the ML.

511   However particles formed close to the surface could probably still be mixed by strong updrafts fast

512   enough so that the number concentrations measured on board the Zeppelin appear homogeneous.

513   The newly formed particles were observed to grow to larger sizes at the same rate within the ML.

514   However, in HTL we observed local enhancements in NPF that were induced by roll vortices in the

515   BL.

516

517   In addition a separate layer of sub-10 nm particles was observed above the ML in HTL. Lampilahti

518   et al. (2020b) showed that such layers in HTL are likely the result of NPF in the topmost part of the

519   RL. Furthermore it was estimated that around 42% of the NPF events observed in HTL at the

520   surface are entrained from such elevated layers. In SPC we observed how NPF could be happening

521   in one air mass but be completely absent in an adjacent air mass with a different origin.

522

523   We presented three case studies (two from Italy and one from Finland). The conditions on our case

524   study days represent the typical conditions in these locations when NPF events usually occur. That

525   is to say, a sunny day with the air masses originating from a certain area during a period of the year

526   (May in HTL and June in SPC) when NPF is common. Nevertheless it is not certain that our case

527   studies represent all NPF event days. NPF events also occur under different kinds of conditions. The

528   growing nucleation mode particles originating from NPF do not always grow smoothly and

529   continuously in the measured size distribution like in our cases, but may have large variation and

530   discontinuities, which may reflect the vertical and horizontal variability in NPF.

531

Atmospheric
Chemistry
and Physics
Discussions

539

540 **Data availability.** Ground-based meteorological data, radiation, gas and particle size distribution

541 data from HTL is available from https://smear.avaa.csc.fi/ (last access: Apr 1, 2021). The Cessna

542 dataset is available from https://doi.org/10.5281/zenodo.3688471 (last access: Oct 23, 2020). The

543 rest of the data used was gathered into another dataset: https://doi.org/10.5281/zenodo.4660145.

544

545 **Author contributions.** HM, TN, SM, ME, IP, SS, JKa, EJ, TYJ, RK, KLeh, SD, AM, RT, DW, FR,

546 TP, TM and MK coordinated the Zeppelin campaign. RV carried out the Cessna measurements. JLa,

547 TN, HM, JKo, KLei and VMK analyzed and interpreted the data. JL and HM prepared the

548 manuscript, with contributions from all coauthors.

549

550 **The authors declare that they have no conflict of interest.**

551

Atmospheric
Chemistry
and Physics
Discussions

552

References

Aalto, P., Hämeri, K., Becker, E., Weber, R., Salm, J., Mäkelä, J. M., Hoell, C., O'Dowd, C. D., Hansson, H.-C., Väkevä, M., Koponen, I. K., Buzorius, G. and Kulmala, M.: Physical characterization of aerosol particles during nucleation events, Tellus B, 53(4), 344–358, doi:10.3402/tellusb.v53i4.17127, 2001.

Camuffo, D., Tampieri, F. and Zambon, G.: Local mesoscale circulation over Venice as a result of the mountain-sea interaction, Bound.-Layer Meteorol., 16(1), 83–92, doi:10.1007/BF02220408, 1979.

Chen, H., Hodshire, A. L., Ortega, J., Greenberg, J., McMurry, P. H., Carlton, A. G., Pierce, J. R., Hanson, D. R. and Smith, J. N.: Vertically resolved concentration and liquid water content of atmospheric nanoparticles at the US DOE Southern Great Plains site, Atmospheric Chem. Phys., 18(1), 311–326, doi:https://doi.org/10.5194/acp-18-311-2018, 2018.

Dal Maso, M., Kulmala, M., Riipinen, I., Wagner, R., Hussein, T., Aalto, P. P. and Lehtinen, K. E.: Formation and growth of fresh atmospheric aerosols: eight years of aerosol size distribution data from SMEAR II, Hyytiälä, Finland, Boreal Environ. Res., 10(5), 323, 2005.

Ehn, M., Junninen, H., Petäjä, T., Kurtén, T., Kerminen, V.-M., Schobesberger, S., Manninen, H. E., Ortega, I. K., Vehkamäki, H., Kulmala, M. and Worsnop, D. R.: Composition and temporal behavior of ambient ions in the boreal forest, Atmospheric Chem. Phys., 10(17), 8513–8530, doi:https://doi.org/10.5194/acp-10-8513-2010, 2010.

Ehn, M., Thornton, J. A., Kleist, E., Sipilä, M., Junninen, H., Pullinen, I., Springer, M., Rubach, F., Tillmann, R., Lee, B., Lopez-Hilfiker, F., Andres, S., Acir, I.-H., Rissanen, M., Jokinen, T., Schobesberger, S., Kangasluoma, J., Kontkanen, J., Nieminen, T., Kurtén, T., Nielsen, L. B., Jørgensen, S., Kjaergaard, H. G., Canagaratna, M., Maso, M. D., Berndt, T., Petäjä, T., Wahner, A., Kerminen, V.-M., Kulmala, M., Worsnop, D. R., Wildt, J. and Mentel, T. F.: A large source of low-volatility secondary organic aerosol, Nature, 506(7489), 476–479, doi:10.1038/nature13032, 2014.

Eisele, F. L. and Tanner, D. J.: Ion-assisted tropospheric OH measurements, J. Geophys. Res. Atmospheres, 96(D5), 9295–9308, doi:10.1029/91JD00198, 1991.

Hakola, H., Tarvainen, V., Laurila, T., Hiltunen, V., Hellén, H. and Keronen, P.: Seasonal variation of VOC concentrations above a boreal coniferous forest, Atmos. Environ., 37(12), 1623–1634, doi:10.1016/S1352-2310(03)00014-1, 2003.

Hamed, A., Joutsensaari, J., Mikkonen, S., Sogacheva, L., Maso, M. D., Kulmala, M., Cavalli, F., Fuzzi, S., Facchini, M. C., Decesari, S., Mircea, M., Lehtinen, K. E. J. and Laaksonen, A.: Nucleation and growth of new particles in Po Valley, Italy, Atmospheric Chem. Phys., 7(2), 355–376, doi:https://doi.org/10.5194/acp-7-355-2007, 2007.

Hari, P. and Kulmala, M.: Station for measuring ecosystem-atmosphere relations (SMEAR II), Boreal Environ. Res., 10(5), 315–322, 2005.

Junninen, H., Ehn, M., Petäjä, T., Luosujärvi, L., Kotiaho, T., Kostiainen, R., Rohner, U., Gonin, M., Fuhrer, K., Kulmala, M. and Worsnop, D. R.: A high-resolution mass spectrometer to measure atmospheric ion composition, Atmospheric Meas. Tech., 3(4), 1039–1053, doi:10.5194/amt-3-1039-2010, 2010.

Kerminen, V.-M., Chen, X., Vakkari, V., Petäjä, T., Kulmala, M. and Bianchi, F.: Atmospheric new particle formation and growth: review of field observations, Environ. Res. Lett., 13(10), 103003, doi:10.1088/1748-9326/aadf3c, 2018.

Kontkanen, J., Järvinen, E., Manninen, H. E., Lehtipalo, K., Kangasluoma, J., Decesari, S., Gobbi, G. P., Laaksonen, A., Petäjä, T. and Kulmala, M.: High concentrations of sub-3nm clusters and frequent new particle formation observed in the Po Valley, Italy, during the PEGASOS 2012 campaign, , doi:http://dx.doi.org/10.5194/acp-16-1919-2016, 2016.

Kulmala, M., Petäjä, T., Nieminen, T., Sipilä, M., Manninen, H. E., Lehtipalo, K., Dal Maso, M., Aalto, P. P., Junninen, H., Paasonen, P., Riipinen, I., Lehtinen, K. E. J., Laaksonen, A. and Kerminen, V.-M.: Measurement of the nucleation of atmospheric aerosol particles, Nat. Protoc., 7(9), 1651–1667, doi:10.1038/nprot.2012.091, 2012.

Kulmala, M., Kontkanen, J., Junninen, H., Lehtipalo, K., Manninen, H. E., Nieminen, T., Petäjä, T., Sipilä, M., Schobesberger, S., Rantala, P., Franchin, A., Jokinen, T., Järvinen, E., Äijälä, M., Kangasluoma, J., Hakala, J., Aalto, P. P., Paasonen, P., Mikkilä, J., Vanhanen, J., Aalto, J., Hakola, H., Makkonen, U., Ruuskanen, T., Mauldin, R. L., Duplissy, J., Vehkamäki, H., Back, J., Kortelainen, A., Riipinen, I., Kurten, T., Johnston, M. V., Smith, J. N., Ehn, M., Mentel, T. F., Lehtinen, K. E. J., Laaksonen, A., Kerminen, V.-M. and Worsnop, D. R.: Direct observations of atmospheric aerosol nucleation, Science, 339(6122), 943–946, doi:10.1126/science.1227385, 2013.

Laakso, L., Grönholm, T., Kulmala, L., Haapanala, S., Hirsikko, A., Lovejoy, E. R., Kazil, J., Kurten, T., Boy, M., Nilsson, E. D., Sogachev, A., Riipinen, I., Stratmann, F. and Kulmala, M.: Hot-air balloon as a platform for boundary layer profile measurements during particle formation, Boreal Environ. Res., 12(3), 279–294, 2007.

Laaksonen, A., Hamed, A., Joutsensaari, J., Hiltunen, L., Cavalli, F., Junkermann, W., Asmi, A., Fuzzi, S. and Facchini, M. C.: Cloud condensation nucleus production from nucleation events at a highly polluted region, Geophys. Res. Lett., 32(6), doi:10.1029/2004GL022092, 2005.

Lampilahti, J., Leino, K., Manninen, A., Poutanen, P., Franck, A., Peltola, M., Hietala, P., Beck, L., Dada, L., Quéléver, L., Öhrnberg, R., Zhou, Y., Ekblom, M., Vakkari, V., Zilitinkevich, S., Kerminen, V.-M., Petäjä, T. and Kulmala, M.: Aerosol particle formation in the upper residual layer, Atmospheric Chem. Phys. Discuss., 1–24, doi:https://doi.org/10.5194/acp-2020-923, 2020a.

Lampilahti, J., Manninen, H. E., Leino, K., Väänänen, R., Manninen, A., Buenrostro Mazon, S., Nieminen, T., Leskinen, M., Enroth, J., Bister, M., Zilitinkevich, S., Kangasluoma, J., Järvinen, H., Kerminen, V.-M., Petäjä, T. and Kulmala, M.: Roll vortices induce new particle formation bursts in the planetary boundary layer, Atmospheric Chem. Phys., 20(20), 11841–11854, doi:https://doi.org/10.5194/acp-20-11841-2020, 2020b.

Lehtipalo, K., Leppä, J., Kontkanen, J., Kangasluoma, J., Franchin, A., Wimmer, D., Schobesberger, S., Junninen, H., Petäjä, T., Sipilä, M., Mikkilä, J., Vanhanen, J., Worsnop, D. R. and Kulmala, M.: Methods for determining particle size distribution and growth rates between 1 and 3 nm using the Particle Size Magnifier, Boreal Environ. Res., 19, 22, 2014.

Leino, K., Nieminen, T., Manninen, H. E., Petäjä, T., Kerminen, V.-M. and Kulmala, M.: Intermediate ions as a strong indicator for new particle formation bursts in boreal forest, Boreal Environ. Res., 21, 274–286, 2016.

Leino, K., Lampilahti, J., Poutanen, P., Väänänen, R., Manninen, A., Buenrostro Mazon, S., Dada, L., Franck, A., Wimmer, D., Aalto, P. P., Ahonen, L. R., Enroth, J., Kangasluoma, J., Keronen, P., Korhonen, F., Laakso, H., Matilainen, T., Siivola, E., Manninen, H. E., Lehtipalo, K., Kerminen, V.-M., Petäjä, T. and Kulmala, M.: Vertical profiles of sub-3 nm particles over the boreal forest, Atmospheric Chem. Phys., 19(6), 4127–4138, doi:10.5194/acp-19-4127-2019, 2019.

Manninen, H. E., Petäjä, T., Asmi, E., Riipinen, N., Nieminen, T., Mikkilä, J., Horrak, U., Mirme, A., Mirme, S., Laakso, L., Kerminen, V.-M. and Kulmala, M.: Long-term field measurements of charged and neutral clusters using Neutral cluster and Air Ion Spectrometer (NAIS), Boreal Environ. Res., 14(4), 591–605, 2009.

Mirme, S. and Mirme, A.: The mathematical principles and design of the NAIS – a spectrometer for the measurement of cluster ion and nanometer aerosol size distributions, Atmospheric Meas. Tech., 6(4), 1061–1071, doi:10.5194/amt-6-1061-2013, 2013.

Nieminen, T., Asmi, A., Dal Maso, M., Aalto, P. P., Keronen, P., Petäjä, T., Kulmala, M. and Kerminen, V.-M.: Trends in atmospheric new-particle formation: 16 years of observations in a boreal-forest environment, Boreal Environ. Res., 19, 191–214, 2014.

Nieminen, T., Yli-Juuti, T., Manninen, H. E., Petäjä, T., Kerminen, V.-M. and Kulmala, M.: Technical note: New particle formation event forecasts during PEGASOS–Zeppelin Northern mission 2013 in Hyytiälä, Finland, Atmospheric Chem. Phys., 15(21), 12385–12396, doi:10.5194/acp-15-12385-2015, 2015.

Nilsson, E. D., Paatero, J. and Boy, M.: Effects of air masses and synoptic weather on aerosol formation in the continental boundary layer, Tellus B, 53(4), 462–478, doi:10.1034/j.1600-0889.2001.530410.x, 2001a.

Nilsson, E. D., Rannik, Ü., Kulmala, M., Buzorius, G. and O'dowd, C. D.: Effects of continental boundary layer evolution, convection, turbulence and entrainment, on aerosol formation, Tellus B, 53(4), 441–461, doi:10.1034/j.1600-0889.2001.530409.x, 2001b.

O'Dowd, C. D., Yoon, Y. J., Junkermann, W., Aalto, P., Kulmala, M., Lihavainen, H. and Viisanen, Y.: Airborne measurements of nucleation mode particles II: boreal forest nucleation events, Atmospheric Chem. Phys., 9(3), 937–944, doi:10.5194/acp-9-937-2009, 2009.

Platis, A., Altstädter, B., Wehner, B., Wildmann, N., Lampert, A., Hermann, M., Birmili, W. and Bange, J.: An Observational Case Study on the Influence of Atmospheric Boundary-Layer Dynamics on New Particle Formation, Bound.-Layer Meteorol., 158(1), 67–92, doi:10.1007/s10546-015-0084-y, 2015.

Schobesberger, S., Väänänen, R., Leino, K., Virkkula, A., Backman, J., Pohja, T., Siivola, E., Franchin, A., Mikkilä, J., Paramonov, M., Aalto, P. P., Krejci, R., Petäjä, T. and Kulmala, M.: Airborne measurements over the boreal forest of southern Finland during new particle formation events in 2009 and 2010, Boreal Environ. Res., 18(2), 145–164, 2013.

Siebert, H., Stratmann, F. and Wehner, B.: First observations of increased ultrafine particle number concentrations near the inversion of a continental planetary boundary layer and its relation to ground-based measurements, Geophys. Res. Lett., 31(9), doi:10.1029/2003GL019086, 2004.

Sipilä, M., Berndt, T., Petäjä, T., Brus, D., Vanhanen, J., Stratmann, F., Patokoski, J., Mauldin, R. L., Hyvärinen, A.-P., Lihavainen, H. and Kulmala, M.: The Role of Sulfuric Acid in Atmospheric Nucleation, Science, 327(5970), 1243–1246, doi:10.1126/science.1180315, 2010.

Sogacheva, L., Hamed, A., Facchini, M. C., Kulmala, M. and Laaksonen, A.: Relation of air mass history to nucleation events in Po Valley, Italy, using back trajectories analysis, Atmos Chem Phys, 7(3), 839–853, doi:10.5194/acp-7-839-2007, 2007.

Sogacheva, L., Saukkonen, L., Nilsson, E. D., Dal Maso, M., Schultz, D. M., De Leeuw, G. and Kulmala, M.: New aerosol particle formation in different synoptic situations at Hyytiälä, Southern Finland, Tellus B, 60(4), 485–494, doi:10.1111/j.1600-0889.2008.00364.x, 2008.

Stein, A. F., Draxler, R. R., Rolph, G. D., Stunder, B. J. B., Cohen, M. D. and Ngan, F.: NOAA's HYSPLIT Atmospheric Transport and Dispersion Modeling System, Bull. Am. Meteorol. Soc., 96(12), 2059–2077, doi:10.1175/BAMS-D-14-00110.1, 2015.

Stull, R. B.: An Introduction to Boundary Layer Meteorology, Softcover reprint of the original 1st ed. 1988 edition., Springer, Dordrecht., 1988.

Väänänen, R., Krejci, R., Manninen, H. E., Manninen, A., Lampilahti, J., Buenrostro Mazon, S., Nieminen, T., Yli-Juuti, T., Kontkanen, J., Asmi, A., Aalto, P. P., Keronen, P., Pohja, T., O'Connor, E., Kerminen, V.-M., Petäjä, T. and Kulmala, M.: Vertical and horizontal variation of aerosol number size distribution in the boreal environment, Atmospheric Chem. Phys. Discuss., Manuscript in review, doi:10.5194/acp-2016-556, 2016.
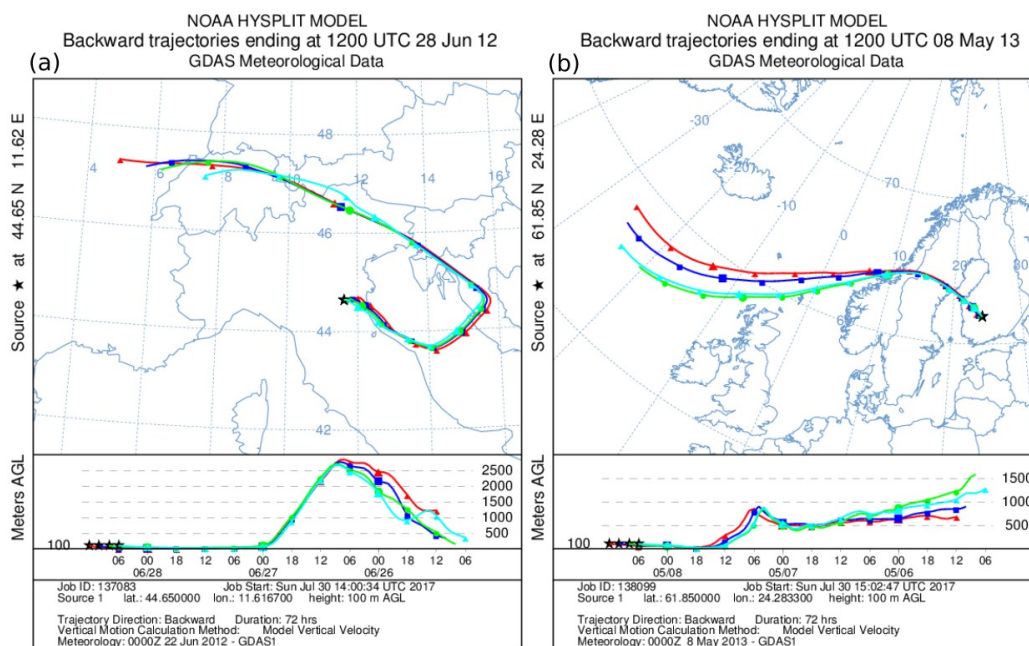
Vanhanen, J., Mikkilä, J., Lehtipalo, K., Sipilä, M., Manninen, H. E., Siivola, E., Petäjä, T. and Kulmala, M.: Particle size magnifier for nano-CN detection, Aerosol Sci. Technol., 45(4), 533–542, doi:10.1080/02786826.2010.547889, 2011.

Wehner, B., Siebert, H., Ansmann, A., Ditas, F., Seifert, P., Stratmann, F., Wiedensohler, A., Apituley, A., Shaw, R. A., Manninen, H. E. and Kulmala, M.: Observations of turbulence-induced new particle formation in the residual layer, Atmospheric Chem. Phys., 10(9), 4319–4330, doi:10.5194/acp-10-4319-2010, 2010.

Wiedensohler, A., Birmili, W., Nowak, A., Sonntag, A., Weinhold, K., Merkel, M., Wehner, B., Tuch, T., Pfeifer, S., Fiebig, M., Fjäraa, A. M., Asmi, E., Sellegri, K., Depuy, R., Venzac, H., Villani, P., Laj, P., Aalto, P., Ogren, J. A., Swietlicki, E., Williams, P., Roldin, P., Quincey, P., Hüglin, C., Fierz-Schmidhauser, R., Gysel, M., Weingartner, E., Riccobono, F., Santos, S., Grüning, C., Faloon, K., Beddows, D., Harrison, R., Monahan, C., Jennings, S. G., O'Dowd, C. D., Marinoni, A., Horn, H.-G., Keck, L., Jiang, J., Scheckman, J., McMurry, P. H., Deng, Z., Zhao, C. S., Moerman, M., Henzing, B., de Leeuw, G., Löschau, G. and Bastian, S.: Mobility particle size spectrometers: harmonization of technical standards and data structure to facilitate high quality long-term observations of atmospheric particle number size distributions, Atmospheric Meas. Tech., 5(3), 657–685, doi:10.5194/amt-5-657-2012, 2012.
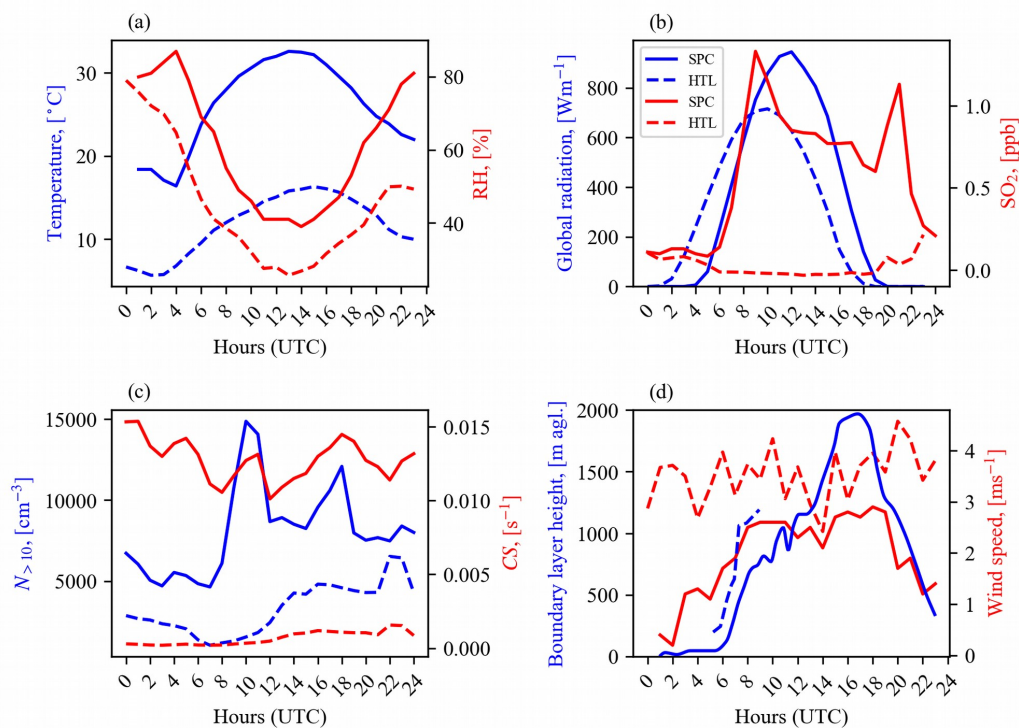
554

555 Figure 1: A schematic diagram of different atmospheric layers in the lower troposphere and their
556 development during the morning hours. A generic Zeppelin measurement profile (dashed gray line)
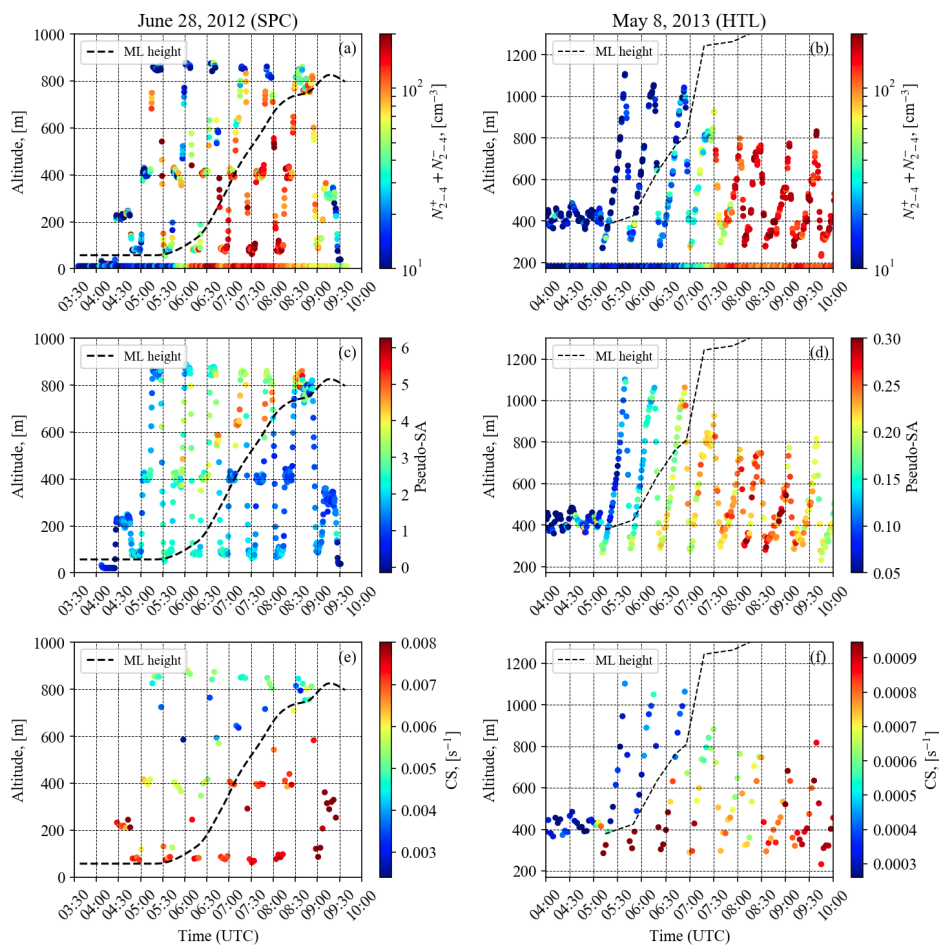557 is displayed on top. The figure is adapted from Stull (1988).
558

559   Figure 2: Airmass backward trajectories to (a) SPC during the morning of June 28, 2012 and (b)
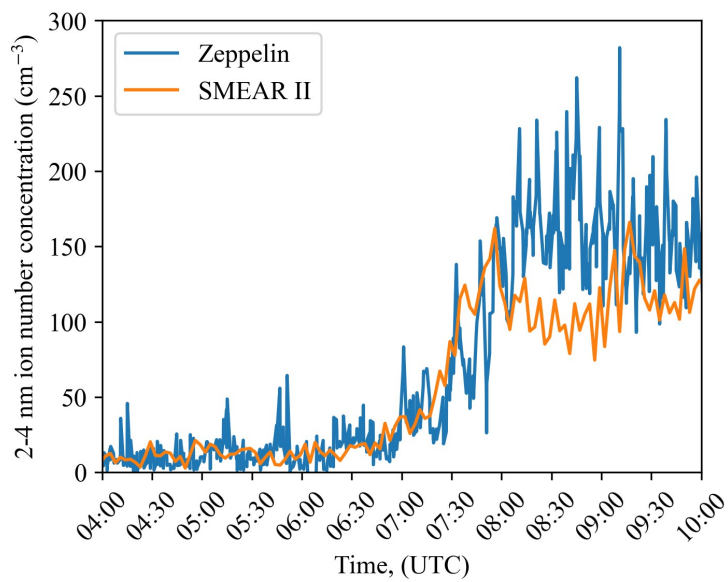560   HTL during the morning of May 8, 2013.

Atmospheric
Chemistry
and Physics
Discussions

Figure 3: Diurnal variation in (a) temperature, relative humidity, (b) global radiation, SO2 concentration, (c) >10 nm particle number concentration, condensation sink (CS) and (d) mixed layer height in SPC on June 28, 2012 and in HTL on May 8, 2013.

Figure 4: Time-evolution of selected variables as a function of height in SPC and HTL. Panels (a) and (b) show the intermediate ion number concentration from SPC and HTL. Ground-based measurements as well as measurements from the Zeppelin are shown. Panels (c) and (d) show the pseudo-SA from SPC and HTL. Panels (e) and (f) show the CS. Height of the mixed layer is shown in all panels.
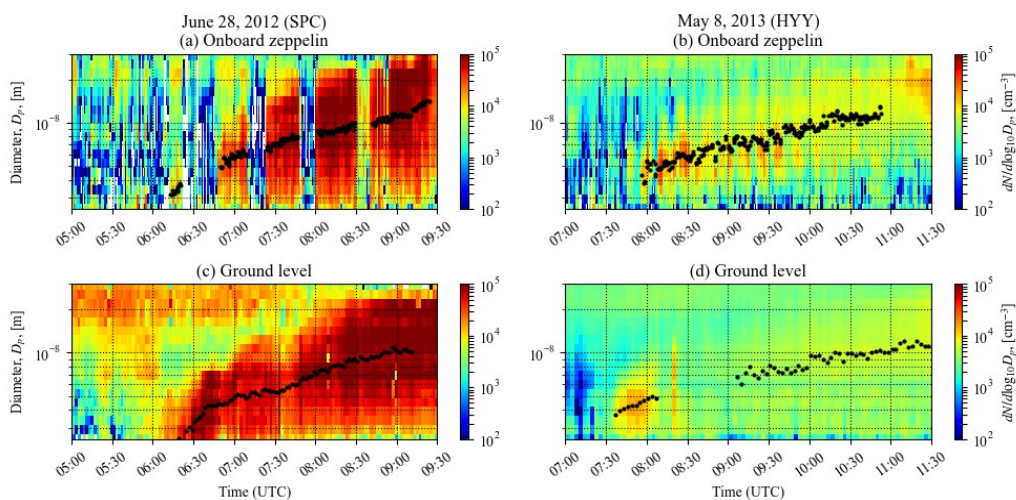
Figure 5: Time series of intermediate (2-4 nm) ion number concentration on board the Zeppelin and the SMEAR II station in HTL on May 8, 2013.
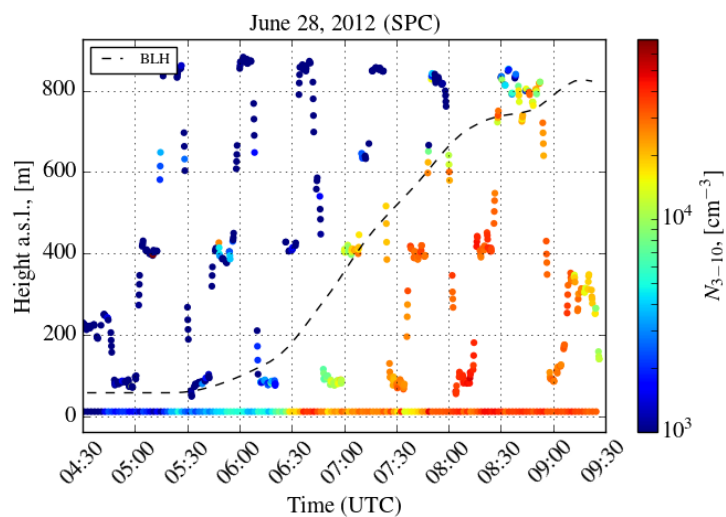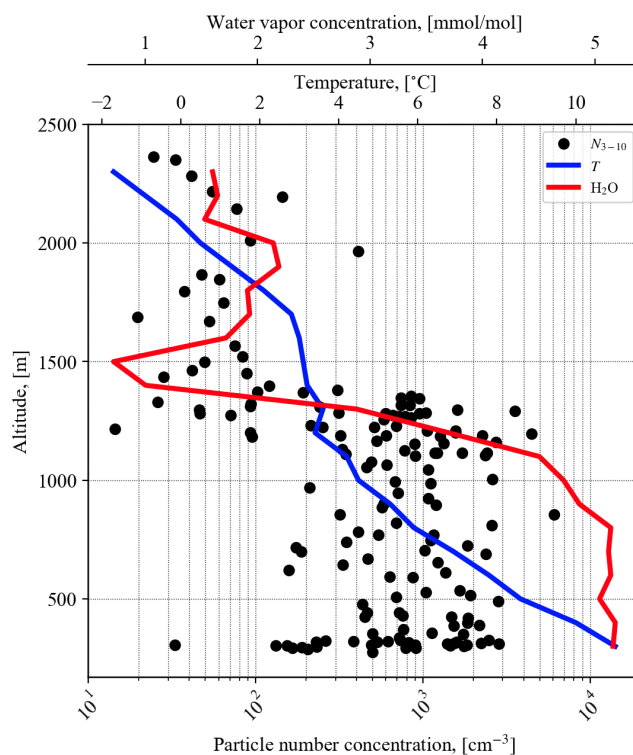
572

573

574 Figure 6. Time evolution of particle number size distributions measured by the NAIS (positive

575 polarity) on board the Zeppelin (a, b) and at the ground level (c, d) in HTL and in SPC on the two

576 case study days. The black dots are the mean mode diameters found by fitting a log-normal

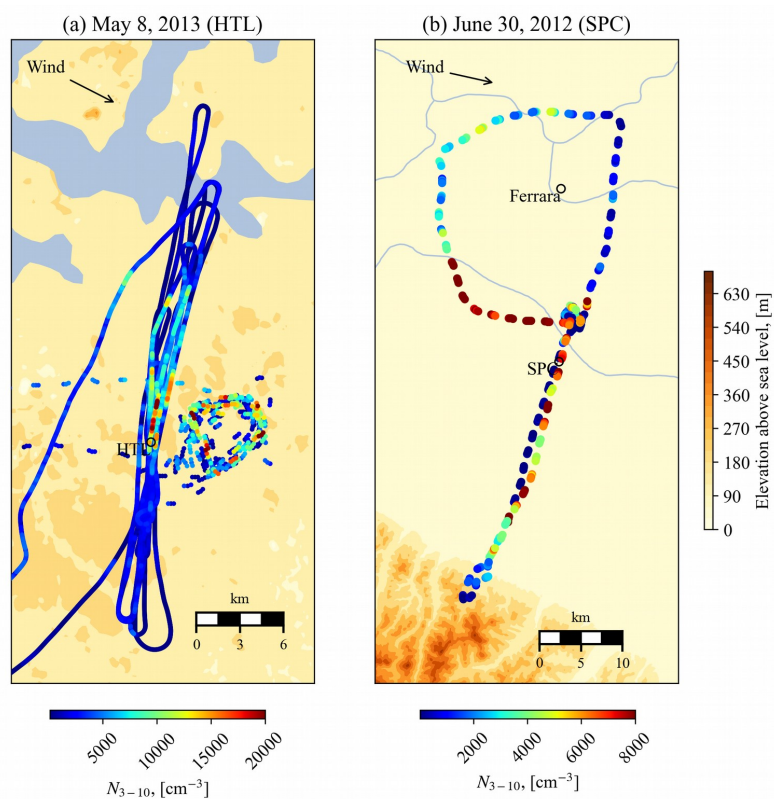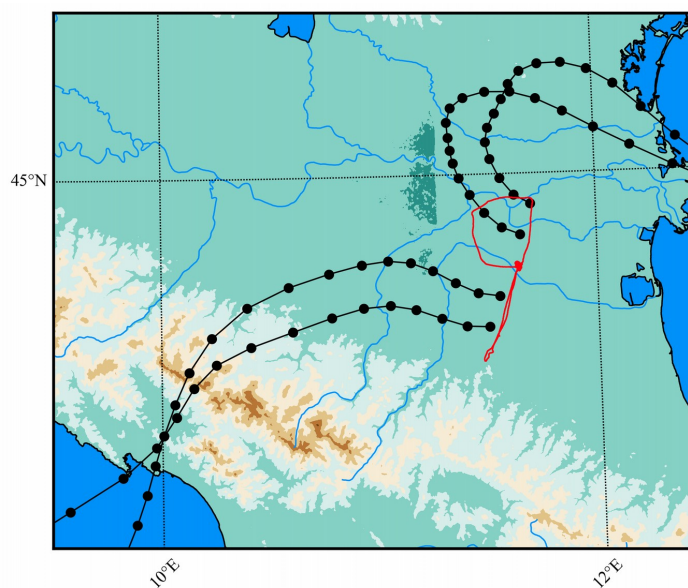577 distribution over the growing mode.

578

579 Figure 7. The particle number concentration in the 3-10 nm size range from SPC on board the
580 Zeppelin and on the ground level on June 28, 2012. BLH refers to the boundary layer height
581 determined from ceilometer.

582

583　Figure 8: Vertical profile of 3-10 nm particle number concentration (black dots), temperature (blue
584　line) and water vapor concentration (red line) measured on board the Cessna between 07:00-10:00
585　on May 8, 2013 in HTL.

Figure 9: (a) the flight tracks of the Zeppelin (circular track) and the airplane (track with back an forth segments) colored by 3-10 nm particle number concentration from HTL on May 8, 2013. (b) the flight track of the Zeppelin colored by 3-10 nm particle number concentration from SPC on June 30, 2012. The Zeppelin flight track has gaps because the NAIS was measuring in the ion mode during that time.

592 Figure 10: Airmass back trajectories (black dotted lines) arriving to the Zeppelin's measurement
593 area over north Italy on June 30, 2012. The separation between the dots along the trajectories is one
594 hour. The red line is the Zeppelin's flight track.

Atmospheric
Chemistry
and Physics
Discussions

595 Table 1. Calculated particle formation and growth rates. + and – superscripts refer to positive and
596 negative ions respectively. The Zeppelin missed the beginning of the NPF event in SPC and because
597 of that some values are missing.
598

	HTL (May 8, 2013)		SPC (June 28, 2012)	
	Zeppelin	Ground	Zeppelin	Ground
$J_{1.5}$, [cm^{-3} s^{-1}]	1.5	0.9	-	-
J_{3}, [cm^{-3} s^{-1}]	0.2	0.3	-	6.8
J_{3}^{-}, [cm^{-3} s^{-1}]	0.04	0.04	-	0.04
J_{3}^{+}, [cm^{-3} s^{-1}]	0.04	0.04	-	0.03
GR_{1-2}, [nm h^{-1}]	0.8	0.7	-	0.5
GR_{2-3}, [nm h^{-1}]	1.4	1.5	1.8	1.5
GR_{3-7}, [nm h^{-1}]	1.7	1.6	2.9	2.0
GR_{7-20}, [nm h^{-1}]	2.4	2.1	3.0	2.8

599